Determination of the CPV Higgs mixing angle in ZZ-fusion at 1.4 TeV CLIC

N. Vukašinović,[a,*] **I. Božović-Jelisavčić,**[a] **G. Kačarević,**[a] **M. Radulović**[b] **and J. Stevanović**[b]

[a] *"VINČA" Institute of Nuclear Sciences - National Institute of the Republic of Serbia, University of Belgrade, Mike Petrovića Alasa 12-14, 11351 Belgrade, Serbia*

[b] *Faculty of Science, University of Kragujevac, Radoja Domanovića 12, 34000 Kragujevac, Serbia*

E-mail: nvukasinovic@vin.bg.ac.rs

In this talk we discuss the CP violation in the Higgs sector under assumption that Higgs is a mixture of CP even and odd states. Study is done in ZZ-fusion production mode, at the intermediate energy stage of CLIC, in full simulation of a detector and machine and physics related backgrounds. By measuring kinematic properties of electron and positron in the final state, in the Higgs exlusive decay to $b\bar{b}$ to reduce backgrounds, we discuss the statistical precision of CP-violating mixing angle measurement with 2.5 ab^{-1} of data.

11th International Conference of the Balkan Physical Union (BPU11),
28 August - 1 September 2022
Belgrade, Serbia

---

[*]Speaker

1. Introduction

Exploring CP violation in the Higgs sector can give an answer to the baryon asymmetry of the Universe as well as provide a sign of a New Physics. In the Standard Model, Higgs boson is a CP even state. CP violation in the Higgs sector can be explored in the extended Higgs sector where mixing of pure CP even (H) and CP odd (A) states can occur:

$$h = H \cdot cos\Psi_{CP} + A \cdot sin\Psi_{CP}, \tag{1}$$

where Ψ_{CP} is the CP violating mixing phase.

At future e^-e^+ Higgs factories there is plethora of possibilities to study CPV in the Higgs sector, either using bosonic (HVV) or fermionic (Hf$\bar{\text{f}}$) vertices (Table 1 [1]).

Table 1: HVV (V = W, Z) and Hf$\bar{\text{f}}$ vertices that can be studied at various center-of-mass energies at future e^-e^+ colliders.

| fermion couplings	
H$\rightarrow \tau^+\tau^-$	250+ GeV
$e^-e^+ \rightarrow Ht\bar{t}$	500+ GeV
boson couplings	
$e^-e^+ \rightarrow HZ$	250+ GeV
H$\rightarrow ZZ$	250+ GeV
H$\rightarrow WW$	250+ GeV
$e^-e^+ \rightarrow He^-e^+$ (ZZ - fusion)	1000+ GeV
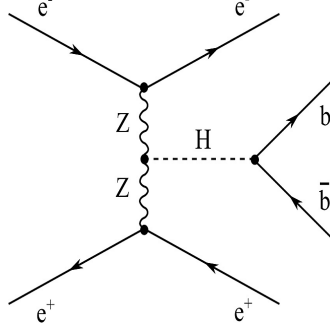
Figure 1: Feynman diagram of the ZZ-fusion where Higgs boson decays to b$\bar{\text{b}}$.

So far, most of the CPV studies are done using Hf$\bar{\text{f}}$ vertices (H$\rightarrow \tau^+\tau^-$ decay and t$\bar{\text{t}}$H production) where CPV factor f$_{CP}$ = $sin^2\Psi_{CP}$ should be measured with the precision of 10^{-2} to meet the theory target [2]. Using bosonic vertices theoretical target is sensitivity to f$_{CP}$ deviations of ~ 10^{-5} determing precision goal of Ψ_{CP} measurement. ILC result in H$\rightarrow \tau^+\tau^-$ decay at 250 GeV with absolute statistical precision of the mixing anlge Ψ_{CP} of $\Delta\Psi_{CP}$ = 75 mrad [3] clearly meets the target. The 2022 Snowmass report on CP violation [2] does not identify CPV analyses in HVV (VV-fusion) vertices.

In this paper we present preliminary results of CPV study in ZZ-fusion at 1.4 TeV CLIC, where Higgs boson decays to $b\bar{b}$ (Figure 1). Aim of the analysis is to determine absolute statistical precision of Ψ_{CP}, for the Standard Model case ($\Psi_{CP} = 0$).

2. CLIC Accelerator and Detector

CLIC accelerator is based on two-beam normal conducting acceleration scheme with acceleration gradient of up to 100 MV/m [4]. It will run in three energy stages (380 GeV, 1.4 (1.5) TeV[1] and 3 TeV, Figure 2 (left) [5]) with more than $3 \cdot 10^6$ Higgs bosons produced in the estimated center-of-mass energy span. Driven by the CLIC physics program, CLICdet [6] detector is optimized for the precision Higgs physics program with all detector subsystems placed within magnetic field of 4 T to enable Particle Flow Algorithm (PFA) [7]. Vertex and tracking detectors are all silicon detectors enabling charge particle reconstruction and identification. Only photons and neutral hadrons are left to be measured at electromagnetic and hadronic calorimeters, respectively. PFA enables jet energy resolution (Figure 2 (right)) in the range of (3-5)% [6], depending on a jet energy of importance for the $b\bar{b}$ final state. Detailed CLICdet performance is discussed in [6].
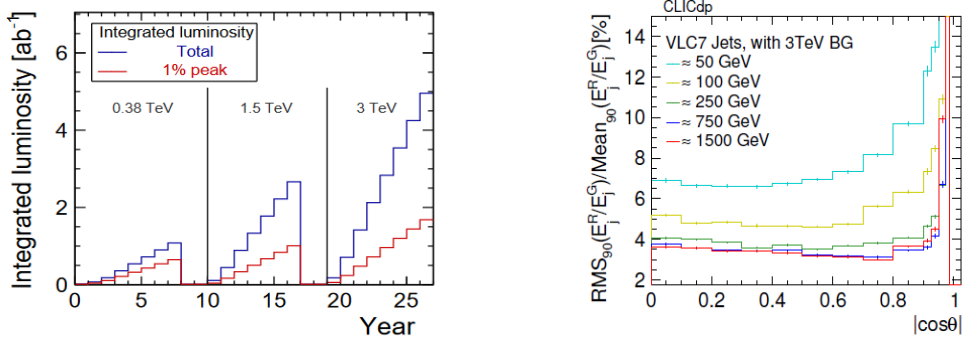

Figure 2: Integrated luminosity of CLIC per energy stage (left). Jet energy resolution for different jet energies as a function of the polar angle ($|\cos\theta|$), in the presence of $\gamma\gamma \rightarrow$ hadron background overlaid on the $Z/\gamma^* \rightarrow q\bar{q}$ events (right).

3. Event selection

We consider exclusive H$\rightarrow b\bar{b}$ decay channel in order to avoid high cross section $e^-e^+ \rightarrow e^-e^+\gamma$ background that is present in inclusive process. As the signal final state is $e^-e^+ + 2$jets: $e^-e^+ \rightarrow He^-e^+(H \rightarrow b\bar{b})$ we select two isolated electrons per event, where the electron is considered isolated if passed cuts on: transverse ($d_0 < 0.04$ mm), longitudinal ($z_0 < 0.1$ mm) and three-dimensional ($R_0 < 0.1$ mm) impact parameters, ratio of energy deposited in electromagnetic and hadronic calorimeters ($E_{ECAL}/(E_{ECAL} + E_{HCAL}) \geq 0.94$) and two-dimensional requirement of cone energy vs. electron energy ($E_{cone}^2 < 9\text{GeV} \cdot E_{trk} + 9\text{GeV}^2$), where the cone energy (E_{cone})

---

[1]Full simulation of real experimental measurement (pseudo-experiment) is done at 1.4 TeV center-of-mass energy that was initially proposed for the second energy stage. Higher center-of-mass energy of 1.5 TeV is chosen subsequently as the maximal center-of-mass energy that can be reached with a single drive-beam complex.

sums up all particle energies in a cone size of approximately 6° around the isolated electron track with energy E_{trk}. Two reconstructed jets determine Higgs boson four-vector. In Figure 3 (left) the Higgs boson invariant mass for the signal and background processes after the selection described above (preselection) is shown. It can be seen that background with large cross section is not completely suppressed. In order to suppress background multivariate analysis (MVA) using sensitive observables is applied, based on the Boosted Decision Tree (BDT) method within the TMVA software package [8]. BDT efficiency is found to be 94%, where a signal efficiency is 81% and the overall background rejection rate is 99.9%. Stackplot of the Higgs boson invariant mass after the MVA is illustrated in Figure 3 (right). It is obtained by restricting the BDT output variable to be larger than 0.16 on event-by-event basis.
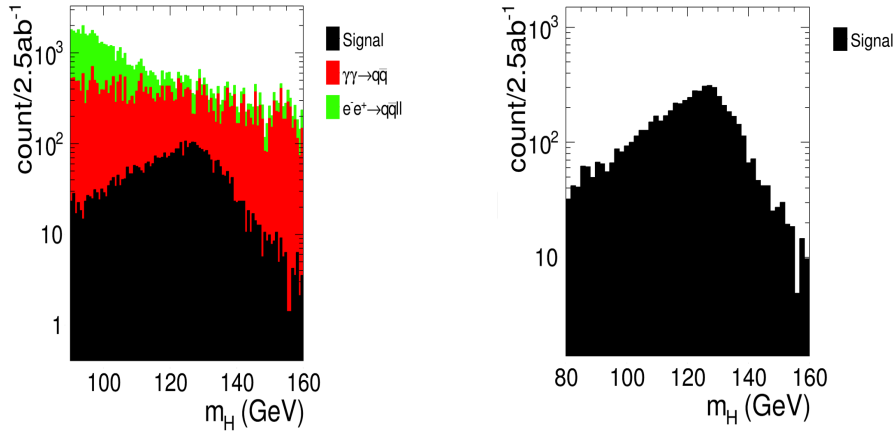
Figure 3: Stackplot of the Higgs boson invariant mass, for signal and background, after the preselection (left) and MVA (right).
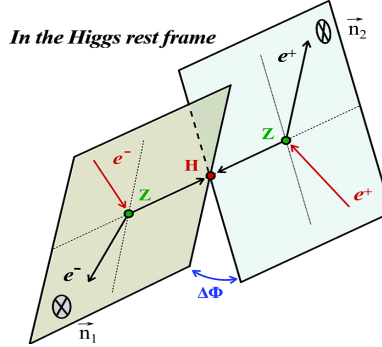
Figure 4: Illustration of the CP sensitive observable $\Delta\Phi$.

4. Sensitive observable

The CPV observable sensitive to scalar-pseudoscalar mixing, is the angle between production planes $\Delta\Phi$ (Figure 4) defined by the initial and final $e^{\pm}$ states and exchanged Z bosons. $\Delta\Phi$ can be

retrieved as the angle between unit vectors ($\vec{n}_1$ and $\vec{n}_2$) orthogonal to these planes:

$$\Delta\Phi = a \cdot \arccos(\vec{n}_1 \cdot \vec{n}_2) \tag{2}$$

where the unit vectors are:

$$\vec{n}_1 = \frac{q_{e_i^-} \times q_{e_f^-}}{|q_{e_i^-} \times q_{e_f^-}|} \qquad \text{and} \qquad \vec{n}_2 = \frac{q_{e_i^+} \times q_{e_f^+}}{|q_{e_i^+} \times q_{e_f^+}|}, \tag{3}$$

a defines how the second (positron) plane is rotated w.r.t. the first (electron) plane; If it falls backwards (as illustrated) $a = -1$, otherwise $a = 1$; Direction of Z in the e^- plane regulates the notion of direction (fwd. or back.) by the right-hand rule. $q_{e_{i,f}^\pm}$ stands for momentum vectors of initial (final) $e^\pm$.
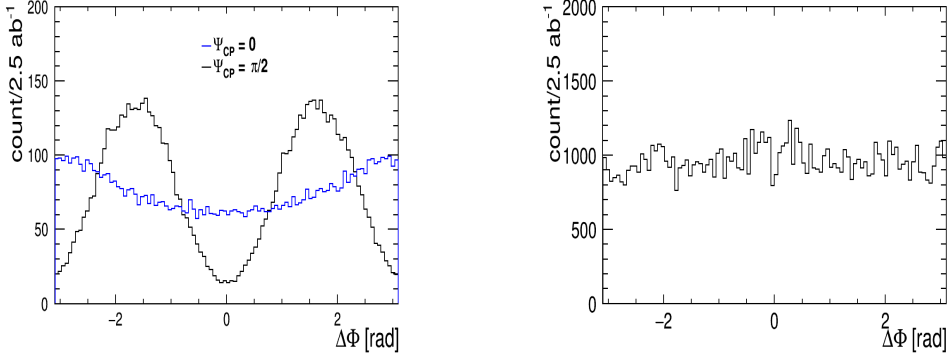
Figure 5: $\Delta\Phi$ distributions at the generator level for pure scalar and pseudoscalar states (left). $\Delta\Phi$ distribution for background after preselection (right).

$\Delta\Phi$ distributions at the generator level for pure scalar and pseudoscalar states are illustrated in Figure 5 (left). Distributions are generated by Whizard generator [9] version 2.8.1 within 2HDM model. It can be seen that these two distributions have different phases regulated by Ψ_{CP}.
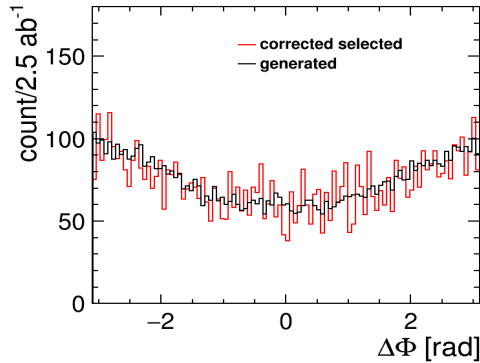
Figure 6: $\Delta\Phi$ for signal after full simulation, reconstruction and selection, corrected for acceptance and detector reconstruction effects (red). Generated distribution (black).

Background is CP insensitive within statistical errors as illustrated in Figure 5 (right) after the preselection phase. After MVA it is suppressed to be negligible. Figure 6 gives reconstructed $\Delta\Phi$ for signal and background corrected for polar angle acceptance effects of the central tracker and for the finite detector resolution. There is ongoing optimization of the fit to extract Ψ_{CP} from the $\Delta\Phi$ distribution. Preliminary fit of $\Delta\Phi$ distribution from Figure 6 indicates the order of magnitude of Ψ_{CP} absolute statistical precision to be $\sim 10^1$ mrad.

5. Conclusion

We give the short overview of the method to measure CPV mixing angle in the Higgs sector where the Higgs mass state is superposition of CP-odd and CP-even states. ZZ-fusion with subsequent H$\rightarrow$ b$\bar{\text{b}}$ decay is considered exclusively at 1.4 TeV CLIC assuming 5.5 ab^{-1} of data. Event selection based on multivariated analysis suppresses background to a negligible level which is otherwise CP insensitive. There is ongoing effort on improvement of the fit method with preliminary sensitivity $< 1°$ of Ψ_{CP} measurement at 1.4 TeV CLIC with 2.5 ab^{-1} of data.

Acknowledgments

References

[1] D. Jeans et al., *Measuring the CP properties of the Higgs sector at electron-positron colliders*, Letter of Interest for SnowMass2021: Energy Frontier (2020).

[2] A. V. Gritsan et. al, *Snowmass White Paper: Prospects of CP-violation measurements with the Higgs boson at future experiments*, arXiv:2205.07715v2 [hep-ex] (2022).

[3] D. Jeans and G. W. Wilson, *Measuring the CP state of tau lepton pairs from Higgs decay at the ILC*, *Phys. Rev.* **D 98** 013007 (2018).

[4] M. Aicheler, P. N. Burrows, N. Catalan Lasheras, R. Corsini, M. Draper, J. Osborne, D. Schulte, S. Stapnes, and M.J. Stuart, *The Compact Linear Collider (CLIC) Project Implementation Plan*, (CERN Yellow Reports: Monographs), CERN-2018-010-M (2018).

[5] P. Roloff and A. Robson, *Updated CLIC luminosity staging baseline and Higgs coupling prospects*, CLICdp-Note-2018-002 (CERN, Geneva, 2018).

[6] D. Arominski et. al [CLICdp Collaboration], *A detector for CLIC: main parameters and performance*, CLICdp-Note-2018-005 (CERN, Geneva, 2018).

[7] M. A. Thomson, *Particle flow calorimetry and the pandora PFA algorithm*, *Nucl. Instrum. Methods Phys. Res., Sect.* **A 611**, 25 (2009).

[8] A. Höcker et al., *TMVA - Toolkit for multivariate data analysis*, arXiv:physics/0703039 (2007).

[9] W. Kilian, T. Ohl, and J. Reuter, *WHIZARD: Simulating multi-particle processes at LHC and ILC*, *Eur. Phys. J.* **C 71**, 1742 (2011).